Hindawi
Journal of Chemistry
Volume 2017, Article ID 3695141, 12 pages
https://doi.org/10.1155/2017/3695141

Research Article

Multivariant Crystallization of Tetraplatin Precursors from Solutions Containing 1,2-$C_6H_{10}(NH_3)_2^{2+}$ and $[PtCl_6]^{2-}$ Ions

R. F. Mulagaleev,[1] D. Y. Leshok,[2] A. K. Starkov,[1] A. N. Matsulev,[1,2] and S. D. Kirik[2]

[1]*Institute of Chemistry and Chemical Technology SB RAS, Krasnoyarsk 660049, Russia*
[2]*Siberian Federal University, Krasnoyarsk 660041, Russia*

Correspondence should be addressed to S. D. Kirik; kiriksd@yandex.ru

Received 6 December 2016; Accepted 15 February 2017; Published 20 June 2017

Academic Editor: Yujiang Song

Seven new phases containing hexachloroplatinate $[PtCl_6]^{2-}$ and trans-1,2-dl-diammoniumcyclohexane 1,2-$C_6H_{10}(NH_3)_2^{2+}$ ions were obtained by crystallization from solutions with minor variation of synthesis conditions. The compounds can be applied as precursors for the synthesis of effective anticancer drug tetraplatin ($[PtC_6H_{10}(NH_2)_2Cl_4]$). The phase diversity was achieved by alterations including solvent acidity, crystallization rate, temperature, type of solvent, and the reagents ratio. The compounds were characterized by chemical and thermal analysis, IR, and ^{1}H NMR spectroscopy. Crystal structures of the five compounds were determined by X-ray powder diffraction technique. The phases have ionic structures involving H_2O, HCl molecules, or Cl^- ions as supplementary species in the lattices. It helps to arrange some frames additionally interconnected by hydrogen bonds between ions and solvent molecules. It was suggested that crystal lattices adapted associated particles presented in solutions. It results in observed variety of the crystal structures. Besides the basic interest the obtained results are important for tetraplatin synthesis control.

1. Introduction

1,2-Diaminocyclohexane tetrachloride platinum (IV) or [Pt(1,2-dach)Cl_4] (where 1,2-dach is d,l-trans-1,2-diaminocyclohexane-$C_6H_{10}(NH_2)_2$), known as ormaplatin or tetraplatin, is an antitumor drug [1–3]. Today, the compound is one of the few platinum drugs, approved for clinical application [4–18]. Tetraplatin is similar to cisplatin on efficiency but has less nephrotoxicity [19]. It was noted to be active against tumors resistant to cisplatin or carboplatin [20]. Tetraplatin can be obtained by the exchange reaction of chloride ligands with 1,2-diaminocyclohexane in platinum salts $K_2[PtCl_4]$ [21] or $K_2[PtCl_6]$ [22] followed by oxidation of Pt(II) to Pt(IV) by the chlorine gas, in case of $K_2[PtCl_4]$. The synthesis can be carried out in 10 hours with the yield less than 55% on platinum. The reaction can be described by Scheme 1.

Recently, a new simple synthetic approach capable of high yield and purity was suggested [23, 24]. The approach consists in the application of soluble precursors as crystalline ionic salts containing anions $[PtCl_6]^{2-}$ and cations 1,2-$C_6H_{10}(NH_3)_2^{2+}$ in 1 : 1 molar ratio. Developing the synthesis it was revealed that the crystallization of the solution with mentioned ionic salt gave a number of distinctive crystalline phases under small variation of the synthetic conditions. As a rule it gave multiphase product. The phenomenon was repeatedly mentioned in the literature [25–30]. Every case has specific features. It impedes a comprehensive control which plays critical role when dealing with the synthesis of important substances such as anticancer drugs. It was the reason why the crystallization stage was separated out from whole synthetic process of the drug and investigated.

It is well known that the synthesis of many complex and organometallic compounds passes through the formation of ionic compounds [31]. The reacting species in a solution can form a variety of spatial associations due to variety of size, shape, charge, presence of hydrogen bond donor, or acceptor. Subsequent crystallization under certain conditions adapts the association of the particles existing in the solution to form crystalline solids. Understanding crystallization features can be used to increase the yield and purity of the required products. Current methods of the solution structure investigation are not able to provide the necessary information

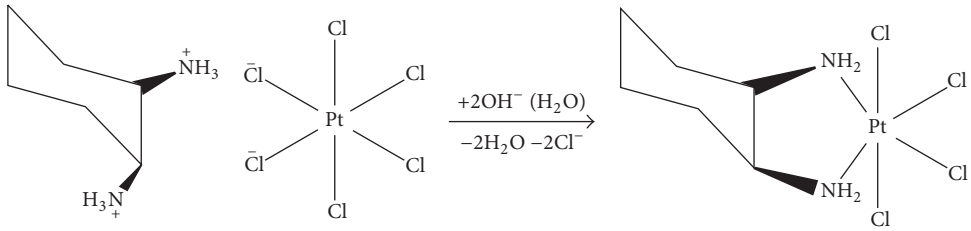

Scheme 1

about the spatial coordination of complex ions. However, crystal structures of precipitated solid phases accept definite imprint of these interactions.

In this work seven new crystalline phases were precipitated from the solutions containing ionic pair $[PtCl_6]^{2-}$ and 1,2-$C_6H_{10}(NH_3)_2^{2+}$ at mild variation of the crystallization conditions. The chemical compositions, thermal stability, IR, and NMR spectra were used for samples characterization. The crystal structures of five compounds have been determined by X-ray powder diffraction technique. The data can be the basis for the interpretation of the particle association at precrystallization state in the solution. Besides the basic interest to the phenomenon of multiphase crystallization the obtained results are important for tetraplatin synthesis controlling.

2. Experimental

All reagents were commercially supplied by "Reahim" (Russia) and "Sigma-Aldrich." Acetone, chloroform, and diethyl ether were purified and dried according to standard procedures [33]. The reagents $H_2[PtCl_6]\cdot 6H_2O$ and $Na_2[PtCl_6]\cdot 6H_2O$ were obtained in accordance with [34]. The integrated scheme of the compound synthesis is presented in Figure 1. The detailed synthesis description and some spectroscopic and chemical composition data are given in supporting information (see Supplementary Materials available online at https://doi.org/10.1155/2017/3695141).

Elemental H, C, N analysis was carried out on Analyzer CHNS-OEA 1108 (Carlo Erba Instruments). The platinum content in compounds was analyzed by heating in air with a gravimetric determination of the residue. Thermal stability was studied using NETZSCH STA 449 thermal analyzer. Decomposition was carried out by heating up to 1073 K in air at the rate 5°/min. IR spectra were recorded in the 400–4000 cm^{-1} region as KBr (0.1%) pellets on Bruker IFS-85 IR spectrophotometer. ^1H NMR data were collected on Bruker Avance 600 spectrometer at 295 K.

3. X-Ray Powder Diffraction Study

The obtained samples were analyzed for crystallinity, single-phase purity, and the possibility of crystal structure determination. The X-ray powder diffraction technique was applied for this purpose. Diffractometer X'Pert PRO (PANalytical) with a PIXcel detector, equipped with a graphite monochromator, was used for scanning X-ray diffraction patterns. CuKα radiation was used. The sample was grinded up in an agate mortar and placed in a cuvette of 25 mm diameter by direct loading with a small pressing. The excess of sample was cut off with a razor to prevent preferred orientation on the surface. Scanning was performed at $T = 295$ K in the range from 3 to 90° 2θ with step 0,026° and Δt-50 c. The angular limit for scanning was caused by the lack of significant diffraction peaks in the high angle region.

Compounds **(I)**–**(VII)** were suitable for diffraction studies. The unit cell search, the cell parameters refinement, and the space group choice were carried out in the programs described in [35, 36]. The structure modeling was completed in the direct space using the "simulated annealing" approach [37], with help of the computer program FOX [38]. The octahedral anionic complex $[PtCl_6]^{2-}$ with the regular geometry and cyclohexane-1,2-diammonium ion in the chair configuration was the basic molecular blocks for the structure modeling. Actually the structure determination consisted in finding an optimal positions and orientations of the molecular particles in the space of a unit cell. The final LS structure optimization was carried out by full-profile analysis (Rietveld method) using the program FullProf [39]. Hard and soft constraints were applied to refined atomic coordinates [40, 41] using the weight coefficients with the average values of distances and angles [1]. Optimization of the structure was done by the gradual removal of restrictions on parallel to the refinement of the background and some profile parameters. Thermal parameters for the platinum and chlorine atoms were refined in the anisotropic approximation but for light atoms in isotropic. At the final step hydrogen atoms were rigidly attached to the respective carbons and nitrogen in a structure model [42]. The resulting structural data have been deposited on CCDC ##1023411–1023415.

4. Results and Discussion

The discussed crystallization phenomena seem to be rather typical but are not well investigated because of the absence of proper samples for crystal structure analysis. There are some common features which define crystal phase formation. On the one hand, there are no significant chemical bonding alterations within the particles in the system, and on the other, the type of the product as a crystalline precipitate in each case has a highly specific identity. The resulting compounds are ionic salts, so their states and relationships must be described in accordance with the chemical thermodynamics using, for example, the phase diagrams. However, some irreversible processes at a chemical phase formation prevent the precise

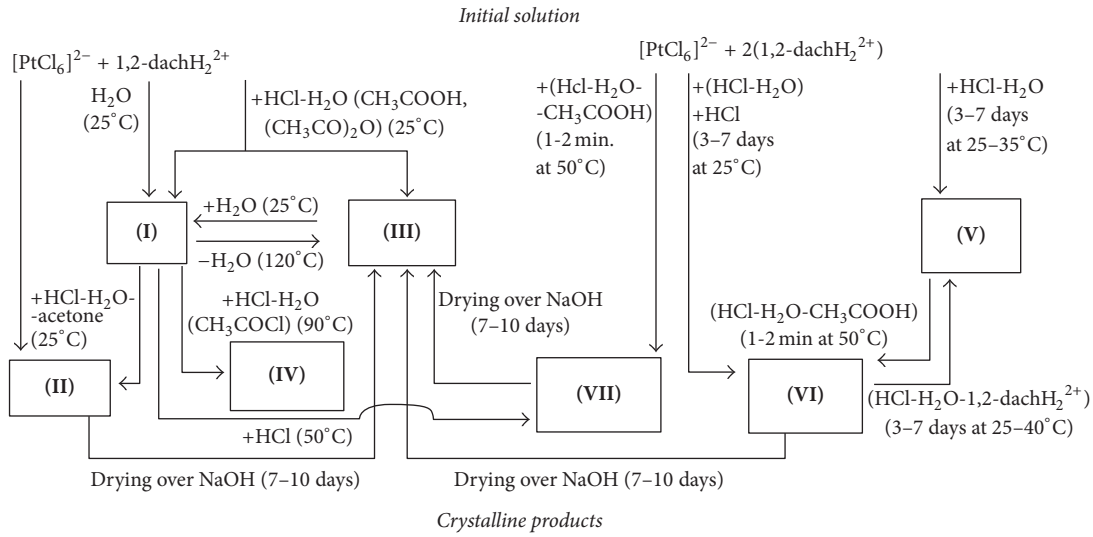

Figure 1: The integrated scheme of phase **(I)**–**(VII)** crystallization depending on synthesis conditions. **(I)** $C_6H_{10}(NH_3)_2[PtCl_6]\cdot H_2O$, **(II)** $C_6H_{10}(NH_3)_2[PtCl_6]\cdot 2HCl$, **(III)** $C_6H_{10}(NH_3)_2[PtCl_6]$, **(V)** $(C_6H_{10}(NH_3)_2)_2[PtCl_6]Cl_2$, and **(VI)** $C_6H_{10}(NH_3)_2[PtCl_6]\cdot HCl$.

compliance with the rules of the classical thermodynamics. In particular, the order of weak hydrogen bonds formation taking place in a solution is important. The control of low-energy alterations in a solution is extremely difficult, and as a consequence, there are insufficient data for phenomena understanding and successful prediction. In the present paper we consider the example of the salt crystallization with cation and anionic pair 1,2-dachH_2^{2+} (where "dachH_2^{2+}" is $C_6H_{10}(NH_3)_2^{2+}$) and $[PtCl_6]^{2-}$ in which small changes in physicochemical conditions significantly diversify the phase formation during crystallization. By adjusting the molar ratio between main components 1,2-dachH_2^{2+} and $[PtCl_6]^{2-}$, changing solution acidity, temperature, rate of crystallization, and varying the type of solvent the crystallization can be directed to any of different compounds shown in Figure 1.

Phase **(I)** formation requires a neutral or slightly acidic solution at the room temperature. Phase **(II)** crystallizes when the aqueous solution is changed into the water-acetone solution in the presence of hydrochloric acid under of slow evaporation conditions. The isoformular compounds **(III)** and **(IV)** can be obtained as a result of solid phase transition of **(I)** in the presence of drying agent such as acetyl chloride or acetic anhydride in glacial acetic acid at elevated temperature. Phase **(V)** crystallization occurs in weak acidic solutions with a molar ratio 1,2-dachH_2^{2+}/$[PtCl_6]^{2-} \geq 2$. The formation of phase **(V)** in a strong acidic solution may be accompanied by coprecipitation of **(VI)** and **(VII)** phases with the ratio of basic ions differing from 1 : 1. However, the crystallization at slow solvent evaporation at 303–333 K leads to the precipitation of pure phase **(V)**. Phase **(VI)** is formed in the temperature range of 293–323 K if hydrochloric acid or glacial acetic acid is added up to the strong acidic solution with molar ratio 1,2-dachH_2^{2+}/$[PtCl_6]^{2-} \geq 1$. If the temperature of the solution is up into the range 323–383 K phase **(VII)** precipitates rapidly.

It is relevant to note that similar experiments performed with respect to organic cations lysinium $(NH_3CH(COOH)(CH_2)_4NH_3)^{2+}$ or 1,4-diammoniumcyclohexane $C_6H_{10}(NH_3)_2^{2+}$ (1,4-dachH_2^{2+}) in the similar range of crystallization conditions have revealed only one distinctive crystalline phase [1]. It indicates the importance of the spatial geometry of the main particles, both in solution and in the solid state.

At heating in air the synthesized phases have the similar stages of decomposition. For example, Figure 2 shows the thermogram for 1,2-(dachH_2)$[PtCl_6]\cdot H_2O$ **(I)**. The first step involves elimination of the solvent molecules. Water completely evaporates up to 423 K. The phases containing HCl start to decompose at 483 K. At 563–573 K the thermal conversion begins by eliminating chlorine and forming complex $[Pt(1,2\text{-dach})Cl_2]$. The last one was determined by X-ray diffraction phase analysis in the intermediate multiphase product of decomposition. Relatively slow transformation stage overlaps the elimination, decomposition, and oxidation of diaminocyclohexane. Platinum dichloride ($PtCl_2$) is the second intermediate product, which decays into metallic platinum at the temperature more than 773 K. The obtained phases are comparable on the thermal stability. Data on the thermal stability of other compounds in comparison with tetraplatin are summarized in the "Supplementary Materials."

The difference between crystalline phases **(I)**–**(VII)** was analyzed by IR spectroscopy. Figure 3 shows IR spectra for phases **(I)**–**(VII)** in comparison with 1,2-dachH_2Cl_2. They have many common details. The bands responsible for (Pt-Cl) vibrations do not fall within considered region. The following assignments of the observed bands can be done: 3110–3160 cm^{-1} [ν(C-H)], 2940–2915 cm^{-1} [$\nu_{as}(CH_2)$], 2870–2845 cm^{-1} [$\nu_s(CH_2)$], 1480–1440 cm^{-1} [$\delta(CH_2)$], and 724–740 cm^{-1} [p(CH_2)]. The main differences are related to (N-H)

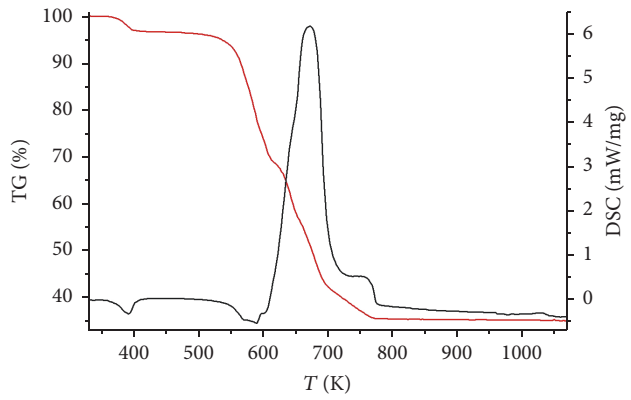

Figure 2: TG and DSC decomposition $C_6H_{10}(NH_3)_2[PtCl_6]\cdot H_2O$ **(I)**.

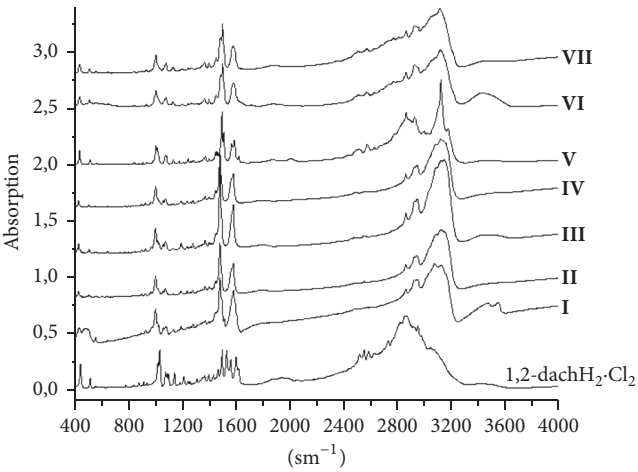

Figure 3: IR spectra of phases **(I)**–**(VII)** and 1,2-dachH_2Cl_2.

oscillations. Bands at 1447–1462 cm^{-1} and 1578–1593 cm^{-1} are assigned to the symmetric deformation vibrations of -NH_3^+ groups. The bands in the regions of 2900–3200 cm^{-1} [ν(N-H)] and 1580–1650 cm^{-1} were assigned to [δ(C-N)] deformation vibrations. Its slight shift to higher frequency for compounds **(I)**–**(VII)** as compared to 1,2-dachH_2Cl_2 occurs due to hydrogen bonding between NH_3^+-groups and chlorine atoms of $[PtCl_6]^{2-}$. The (Pt-N) oscillation at 480 cm^{-1} was not observed [43]. It proves the absence of platinum coordinated by nitrogen atom.

The important information, respectively, the presence of solvent molecules in the crystal structures, was obtained using two-dimensional ^{1}H NMR solid state spectroscopy on the examples of two phases **(I)** and **(II)**. Figures 4(a), 4(b), and 4(c) show its two-dimensional ^{1}H NMR spectra in comparison with $C_6H_{10}(NH_3)_2Cl_2$. There are two spots corresponding to -NH_3^+ and -CH_2 groups of the organic cation $C_6H_{10}(NH_3^+)_2$ on the diagonal of the spectrum for $C_6H_{10}(NH_3)_2Cl_2$ (Figure 4(a)). Spot asymmetry and elongation in the two-dimensional graph cause the splitting of spectral bands belonging to hydrogen atoms of carbon and nitrogen due to the structural nonequivalence of nuclei.

In the spectrum of the complex salt $C_6H_{10}(NH_3)_2[PtCl_6]\cdot H_2O$ **(I)** (Figure 4(b)) there is an additional peak located between the peaks of -NH_3^+ and -CH_2 groups, which should be attributed to the protons of the water molecule. The appearance of new spots out of the main diagonal indicates interaction of water molecules with -NH_3^+ groups. It is reasonable to assume the formation of hydrogen bonds between NH_3^+ groups and oxygen of water molecules. The presence of hydrogen bonds is evidenced by the deformation of the NH_3^+ spot too. However hydrogen atoms of water molecules are not involved in hydrogen bonding.

^{1}H NMR spectrum and two-dimensional pattern for phase $C_6H_{10}(NH_3)_2[PtCl_6]\cdot 2HCl$ **(II)** are depicted in Figure 4(c). The number of spots on the main diagonal becomes equal to four. It means the presence of two unequal protons additionally. Free chlorine atoms strongly influence the protons of NH_3^+ groups and induce significant peak overlapping. It is reasonable to attribute two additional protons to nonequivalent HCl molecules in the structure. It well corresponds to structural data and proves that HCl molecules are involved into the structure.

Crystal structures of $C_6H_{10}(NH_3)_2[PtCl_6]\cdot H_2O$ **(I)**, $C_6H_{10}(NH_3)_2[PtCl_6]\cdot 2HCl$ **(II)**, $C_6H_{10}(NH_3)_2[PtCl_6]$ **(III)**, $(C_6H_{10}(NH_3)_2)_2[PtCl_6]Cl_2$ **(V)**, and $C_6H_{10}(NH_3)_2[PtCl_6]\cdot HCl$ **(VI)** were determined by X-ray powder diffraction technique. Because of impurities in the substances the final results for phases **(IV)** and **(VII)** were not obtained. Some experimental data and characteristics of the crystal structures after refinement are collected in Table 1. Figures 5(a), 5(b), 5(c), 5(d), and 5(e) show the X-ray diffraction patterns (Rietveld's plots), including experimental and calculated diffraction patterns in comparison, the difference between them, and the reflections position. Structures of the compounds in the projection on the (*ac*)-plane are also shown in Figures 5(a), 5(b), 5(c), 5(d), and 5(e). The basic bond lengths and angles are collected in Table 2.

Investigated substances have ionic structure. It may be suggested that Coulomb forces determine the most advantageous configuration for ions packing. However, there are at least two other additional factors influencing packing. The first factor relates to the ion shapes and charge distribution in polyatomic particles. Ions $C_6H_{10}(NH_3)_2^{2+}$ and $[PtCl_6]^{2-}$ are significant in size and different in shape. The $[PtCl_6]^{2-}$ anion has high molecular symmetry (O_h), but it is unlikely that the symmetry of the electric field is of the central character. In the ideal case the symmetry of $C_6H_{10}(NH_3)_2^{2+}$ cation is limited by twofold axis (C_2). Apparently the cations lose this poor symmetry in the lattice. The second factor deals with the localization of donors and acceptors of hydrogen bonds. It plays considerable role in the association of the ions into various groups. The mentioned factors essentially reduce the influence of the Coulomb forces on packing geometry. The "packing factor" presented in Table 1 reflects the variable role of the discussed factors on crystal structures. In the studied crystal structures the layers formed by alternating cation-anion pairs can be distinguished. Noticeable structural variation can be reduced to some shifts of adjacent layers relatively each other. Different layer shifts induce different

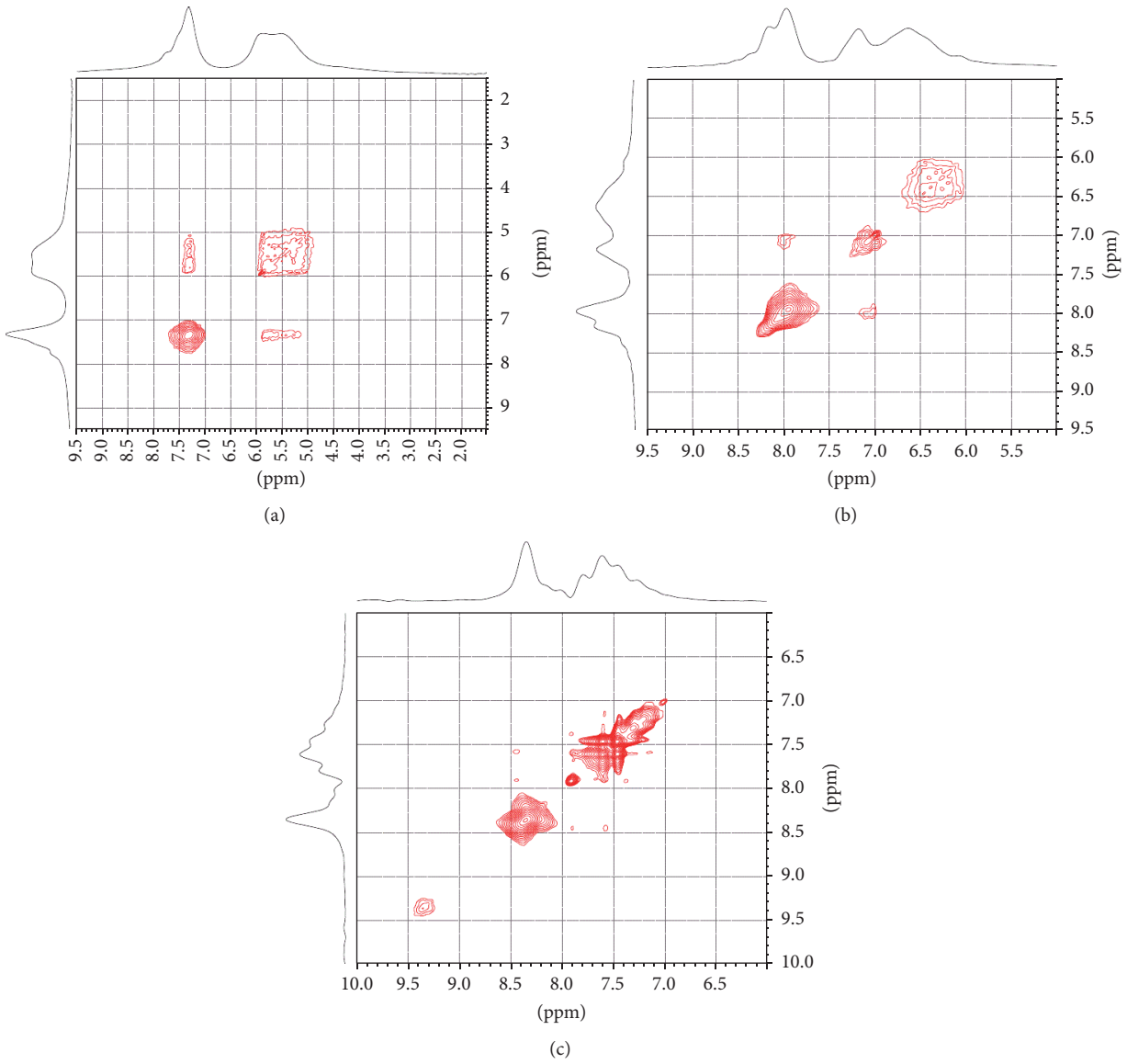

Figure 4: Two-dimensional ^{1}H NMR spectra of phases: (a) $C_6H_{10}(NH_3)_2Cl_2$, (b) **(I)**, and (c) **(II)**.

variants of anion surrounding with a variable number of cations $C_6H_{10}(NH_3)_2^{2+}$. Every anion in compounds **(I)**–**(III)** is coordinated by 4 cations and in **(V)** and **(VI)** by 6 and 3, respectively. The shortest distances between Pt and the center of cyclohexane ring are in the range of 5.1–5.8 Å. The ion packing in the layers can be characterized as separate for **(I)** and **(II)** and as a ribbon for **(III)**–**(VI)** compounds.

A symmetry of a cation-anion pair determines point and ultimately a space group. For compounds **(I)**–**(III)** with the monoclinic crystal system, there are no ion locations on the symmetry elements and particles uniformly fill the volume of the unit cell. Phase **(VI)** has orthorhombic unit cell. $[PtCl_6]^{2-}$ anions, $C_6H_{10}(NH_3)_2^{2+}$ cations and HCl molecules are located on the 2-fold axes.

Dipole molecules of the solution play special role in the crystal structure formation of **(I)**, **(II)**, **(V)**, and **(VI)**. They associate with $C_6H_{10}(NH_3)_2^{2+}$ forming hydrogen bonds via the NH_3-groups. Some associates can be pointed out: $C_6H_{10}(NH_3)_2^{2+}\cdot HCl$, $(C_6H_{10}(NH_3)_2^{2+}\cdot Cl^-)$ or $C_6H_{10}(NH_3)_2^{2+}\cdot H_2O$. Oxygen or chlorine atoms orient towards NH_3-groups. The distances N···O and N···Cl^- are shorter than N···Cl formed between nitrogen and chlorines belonging to anionic complex $[PtCl_6]^{2-}$ (Table 3).

The spatial configurations of associated particles in the investigated structures are presented in Figures 6(a), 6(b), 6(c), 6(d), and 6(e). A number of features can be identified considering the structures of phases **(I)**, **(II)**, and **(VI)** with neutral molecules HCl or H_2O. Phase $C_6H_{10}(NH_3)_2[PtCl_6]\cdot H_2O$ **(I)** was obtained at rapid crystallization (a few minutes) in neutral medium. The contact between cation $C_6H_{10}(NH_3)_2^{2+}$ and neutral molecule of water is provided by one hydrogen bond (O···H-N)

Table 1: Crystal data and experimental conditions for compounds **(I)**–**(VII)**.

Chemical formula	$C_6H_{10}(NH_3)_2$ $[PtCl_6]\cdot H_2O$ **(I)**	$C_6H_{10}(NH_3)_2$ $[PtCl_6]\cdot 2HCl$ **(II)**	$C_6H_{10}(NH_3)_2$ $[PtCl_6]$ **(III)**	$C_6H_{10}(NH_3)_2$ $[PtCl_6]$ **(IV)**	$(C_6H_{10}(NH_3)_2)_2$ $[PtCl_6]Cl_2$ **(V)**	$C_6H_{10}(NH_3)_2$ $[PtCl_6]\cdot HCl$ **(VI)**	$C_6H_{10}(NH_3)_2$ $[PtCl_6]\cdot HCl$ **(VII)**
Molecular weight	539.99	594.89	523.99	523.99	711.10	559.44	559.44
Space group	*C2*	$P2_1/a$	$P2_1$	$P2_1mn$	$P2_1/n$	*Pnn2*	$P2_1$
a, Å	19.9191 (8)	19.2877 (7)	12.6166 (2)	6.9984 (6)	11.5373 (5)	6.9885 (5)	16.2364 (1)
b, Å	7.8461 (6)	9.9590 (3)	6.9987 (7)	8.4936 (8)	6.8973 (7)	7.6583 (2)	15.8851 (1)
c, Å	9.7954 (7)	10.3785 (5)	8.4963 (5)	12.6049 (6)	16.0269 (5)	18.1828 (5)	7.6522 (6)
α, (°)	90	90	90	90	90	90	90
β, (°)	91.004 (4)	92.062 (5)	91.393 (9)	90	94.883 (1)	90	98.028 (1)
γ, (°)	90	90	90	90	90	90	90
$V_{\text{unit cell}}$, Å^3	1530.7 (2)	1992.28 (8)	750.00 (1)	749.26 (1)	1270.73 (1)	973.14 (7)	1954.30 (1)
Z	4	4	2	2	2	2	4
V/*Z*, Å^3	382.6 (8)	498.07 (2)	375.00 (1)	374.63 (1)	635.36 (5)	486.57 (3)	488.57 (5)
$\rho_{\text{calc.}}$, g/cm^3	2.343	1.983	2.320		1.859	1.909	
Packing index [32]	68.9	59.1	64.9		63.9	56.2	
μ, mm^{-1}	26.665	22.932	27.130		18.117	22.191	
T, K	295	295	295	295	295	295	295
Diffractometer	X'Pert PRO	X'Pert PRO	X'Pert PRO	X'Pert PRO	X'Pert PRO	X'Pert PRO	X'Pert PRO
Radiation	Cu Kα	Cu Kα	Cu Kα	Cu Kα	Cu Kα	Cu Kα	Cu Kα
λ *K*α*1*, Å	1.54056,	1.54056,	1.54056,	1.54056,	1.54056,	1.54056,	1.54056,
λ *K*α*2*, Å	1.54439	1.54439	1.54439	1.54439	1.54439	1.54439	1.54439
Scan area, 2θ (°)	3.039–80.935	3.039–80.935	3.013–80.935	3.013–80.909	5.079–100.967	3.013–71.965	3.013–80.935
Number of points	2996	2996	2997	2997	3688	2652	2997
Number of reflections	951	1244	930		1331	451	
R_p, %	7.33	7.81	5.56		8.92	8.23	
R_{wp}, %	10.60	10.90	7.62		12.10	11.60	
R_{exp}, %	5.66	7.63	4.97		6.27	7.87	
R_B, %	4.23	4.35	3.56		4.71	4,52	
$S = R_{\text{wp}}/R_{\text{exp}}$	1.87	1.42	1.53		1.92	1.47	

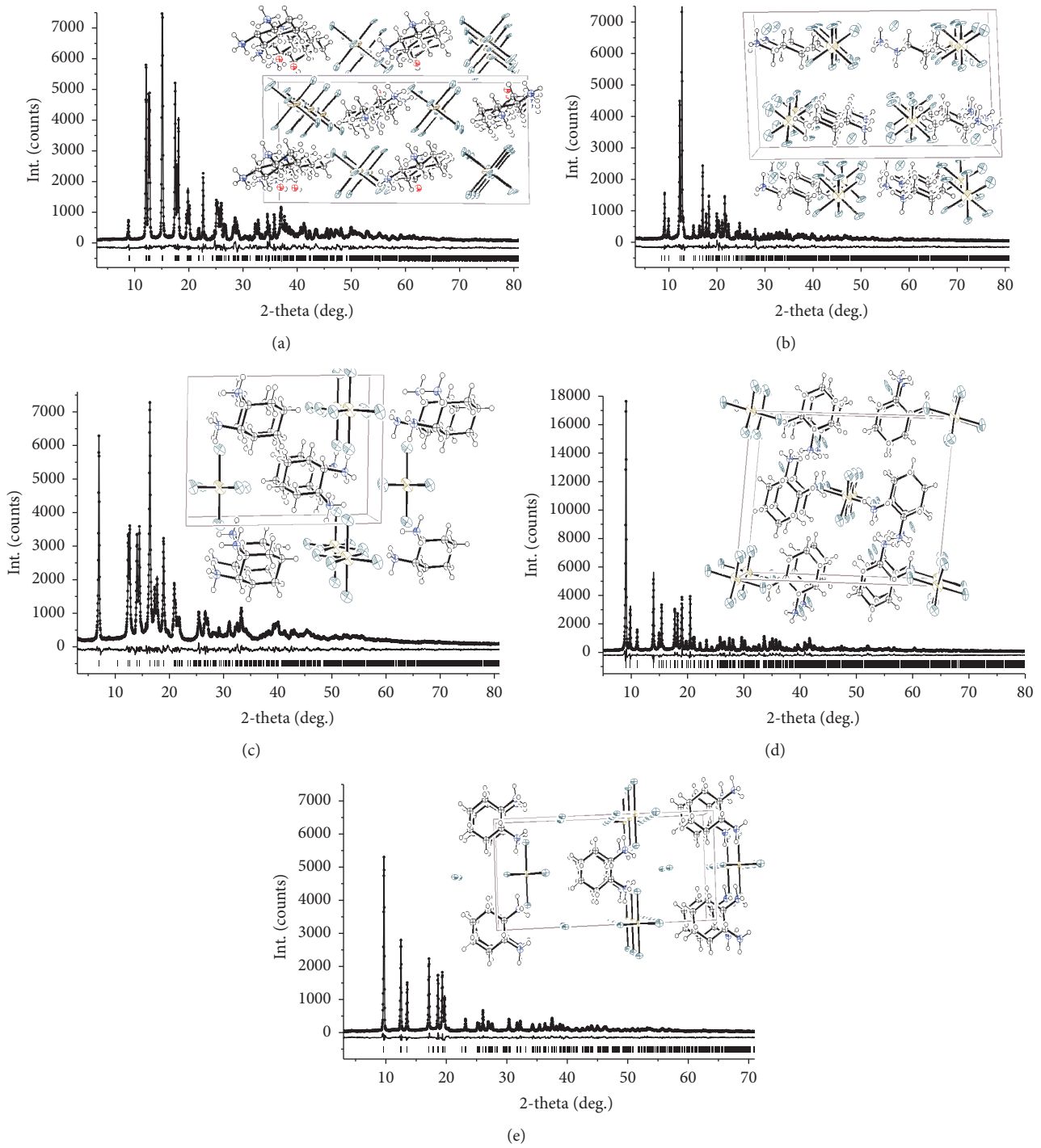

FIGURE 5: Crystal structures and Rietveld plots of the investigated compounds. (a) $C_6H_{10}(NH_3)_2[PtCl_6]\cdot H_2O$ **(I)**, (b) $C_6H_{10}(NH_3)_2[PtCl_6]\cdot 2HCl$ **(II)**, (c) $C_6H_{10}(NH_3)_2[PtCl_6]$ **(III)**, (d) $(C_6H_{10}(NH_3)_2)_2[PtCl_6]Cl_2$ **(V)**, and (e) $C_6H_{10}(NH_3)_2[PtCl_6]\cdot HCl$ **(VI)**.

(d = 2.45 Å) (Figure 6(a)). Charged centers of the cation do not locate on the line between the anion and the center of the cation. It can be reasonably assumed that the species of $C_6H_{10}(NH_3)_2{}^{2+}\cdot H_2O$-type participate in the crystallization. The packing seems to obey the principle of dense space filling rather than the orientation according to electric field. The situation is somewhat different for phase **(II)**. HCl molecule differs from H_2O due to the possibility of easy dissociation just in the crystal structure. As a result, the charge compensation of the cation can be achieved at the less cost than involving big anion as $[PtCl_6]^{2-}$. Additionally the hydrogen bonds are formed. Apparently, the energy gain

Table 2: Some of the bond lengths and angles in compounds **(I)**–**(III)**, **(V)**, and **(VI)**.

d(A-B), Å	**(I)**	**(II)**	**(III)**	**(V)**	**(VI)**
Pt-Cl1	2.25 (1)	2,22 (2)	2.22 (2)	2.24 (1)	
Pt-Cl2	2.25 (1)	2.23 (2)	2.19 (1)	2.25 (1)	2.25 (1)
Pt-Cl3	2.26 (1)	2.24 (2)	2.25 (1)	2.29 (1)	2.25 (1)
Pt-Cl4	2.27 (1)	2.25 (1)	2.19 (1)		2.23 (2)
Pt-Cl5	2.27 (2)	2.23 (1)	2.23 (1)		
Pt-Cl6	2.25 (1)	2.22 (1)	2.20 (1)		
C1-C2	1.54 (1)	1.54 (1)	1.54 (1)	1.54 (1)	1.53 (1)
C1-N1	1.46 (1)	1.46 (1)		1.49 (1)	1.46 (1)
C2-N2	1.49 (2)	1.48 (1)		1.48 (2)	
d(A-B-C), °	**(I)**	**(II)**	**(III)**	**(IV)**	**(V)**
Cl1-Pt-Cl2	89.9 (2)	92.2 (1)	90.2 (1)	90.5 (1)	
Cl2-Pt-Cl3	89.9 (1)	87.6 (1)	89.7 (1)	90.4 (1)	90.1 (1)
Cl4-Pt-Cl3	90.4 (1)	87.5 (2)	91.0 (1)		89.9 (1)
Cl4-Pt-Cl5	89.8 (2)	91.9 (2)	89.8 (1)		
Cl5-Pt-Cl6	89.9 (2)	87.9 (1)	90.2 (2)		
Cl1-Pt-Cl6	90.0 (1)	87.6 (1)	90.5 (1)		
N1-C1-C2	114.5 (1)	111.4 (1)		113.4 (1)	114.7 (2)
C1-C6-C5	112.0 (1)	111.7 (1)	111.6 (1)	113.1 (1)	

arises from the introduction of the second HCl molecule, which dissociates and compensates the electric field. Definitely identified hydrogen bonds occurred between HCl and cation $C_6H_{10}(NH_3)_2^{2+}$ as shown in Figure 6(b). It is relevant to note that the crystallization of the compound with two water molecules does not occur.

Phase 1,2-dachH_2[$PtCl_6$]·HCl **(VI)** occurs as a result of competition for incorporation into the lattice between the cation $C_6H_{10}(NH_3)_2^{2+}$, being in double excess, and the HCl molecule in solution. Due to the reasons described above HCl molecule wins in this competition. Its role in the structure is to reduce electric field. It is implemented during the formation of the layer which consisted of Cl^{1-} anions (Figure 6(e)). The system of hydrogen bonds between pairs of $C_6H_{10}(NH_3)_2^{2+}$ and $[PtCl_6]^{2-}$ presents a zigzag chain (Figure 6(e)). It should be also noted there is the correlation between the presence of HCl in the crystal structure and the "packing index" (Table 1).

Phase **(V)** can be attributed to double salts with 1,2-dachH_2[$PtCl_6$] and 1,2-dachH_2Cl_2 cocrystallized in mutual lattice. Cations are the same but anions are strongly different in size. It is surprising, but the anions form the joint sublattice. The structure has the most saturated system of hydrogen bonds which are responsible for connecting the ions within the layers. Every amine group forms three different H-bonds with chlorine atoms from neighboring anions. Cations 1,2-dachH_2^{2+} are oriented relatively $[PtCl_6]^{2-}$ complexes as well as Cl^- ions (Figure 6(d)).

Phase **(III)**, unlike all previous ones, does not contain solvent molecules in the structure. This is certainly a consequence of its preparation procedure. The absence of solvent molecules in the crystal structure leads to the formation of more dense packing in comparison with other phases. Counterions orientate towards each other by their electron donating and electron accepting centers. It makes possible the formation of hydrogen bonds. Half of the chlorine atoms of $[PtCl_6]^{2-}$ anions are involved in hydrogen bonding (Figure 6(c)), which form zigzag chains. From a thermodynamic point of view, phase **(III)** is an unstable compound. As mentioned above, phase **(III)** transforms into **(I)** in the air. This indicates benefit from the inclusion of solvent molecules in the structure.

The investigated phase formation in the ionic system 1,2-$C_6H_{10}(NH_3)_2^{2+}$-$[PtCl_6]^{2-}$ leads to the number of conclusions. The diversity of crystalline forms in the system is due to the peculiarities of the ions structure. Basically dissimilar symmetry and shape of $[PtCl_6]^{2-}$ and $C_6H_{10}(NH_3)_2^{2+}$ ions, significant charge, and predisposition to dissolution are prerequisites for crystallization of various types of packaging, with negligible energetic difference of the crystal lattices. This fact is confirmed by similar interionic distances in the crystal structures. Due to the presence of donors and acceptor of hydrogen bonds, there is the possibility of hydrogen bonding in the crystal structures and even in the solution. The hydrogen bonds established in solution affect the direction of crystallization. Small alterations in the solution relating to individual components of the solvent, pH, and temperature may provide a path of the crystallization terminated by one of the possible crystals.

5. Conclusion

The crystallization of the ionic salts from the solution containing $[PtCl_6]^{2-}$ and 1,2-$C_6H_{10}(NH_3)_2^{2+}$ ions was investigated at varied conditions including solvent acidity, crystallization rate, reactants mole ratio, temperature, and type of

Table 3: The lengths of the suggested hydrogen bonds in compounds **(I)**–**(III)**, **(V)**, and **(VI)** in Å.

$C_6H_{10}(NH_3)_2[PtCl_6]\cdot H_2O$ **(I)**	$C_6H_{10}(NH_3)_2[PtCl_6]\cdot 2HCl$ **(II)**	$C_6H_{10}(NH_3)_2[PtCl_6]$ **(III)**	$(C_6H_{10}(NH_3)_2)_2[PtCl_6]Cl_2$ **(V)**	$C_6H_{10}(NH_3)_2[PtCl_6]\cdot HCl$ **(VI)**
(N2-H$\cdots$O$^{(i)}$) - 2.45 (1) (N1-H$\cdots$Cl5$^{(i)}$)- 2.88 (1).	(N1-H$\cdots$Cl7$^{(i)}$) - 2.96 (1)	(N1-H$\cdots$Cl4$^{(i)}$) - 2.83 (1). (N2-H$\cdots$Cl1$^{(ii)}$) - 2.93 (1).. (N2-H$\cdots$Cl2$^{(ii)}$) - 2.93 (1).	(N1-H$\cdots$Cl2$^{(i)}$) - 2.85 (1). (N1-H$\cdots$Cl4$^{(ii)}$) - 2.69 (2). (N2-H$\cdots$Cl2$^{(iii)}$) - 3.18 (1). (N2-H$\cdots$Cl3$^{(iv)}$) - 3.26 (1). (N2-H$\cdots$Cl4$^{(v)}$) - 3.11 (1). (N1-H$\cdots$Cl4$^{(vi)}$) - 2.84 (1).	(N4-H$\cdots$Cl2$^{(i)}$) - 3.09 (1).
(i) "$x, y-1, z$"	(i) "$-x, 1-y, 1-z$"	(i) "$1+x, y, z$" (ii) "$-x, y+3/2, 2-z$"	(i) "$1-x, 1-y, 1-z$"; (ii) "$x, 1+y, z$"; (iii) "$1/2+x, 3/2-y, 1/2+z$"; (iv) "$1/2-x, 1/2+y, 1/2-z$"; (v) "$x, 1+y, z$"; (vi) "$3/2-x, 1/2+y, 3/2-z$"	(i) "$1-x, 1-y, -z$"

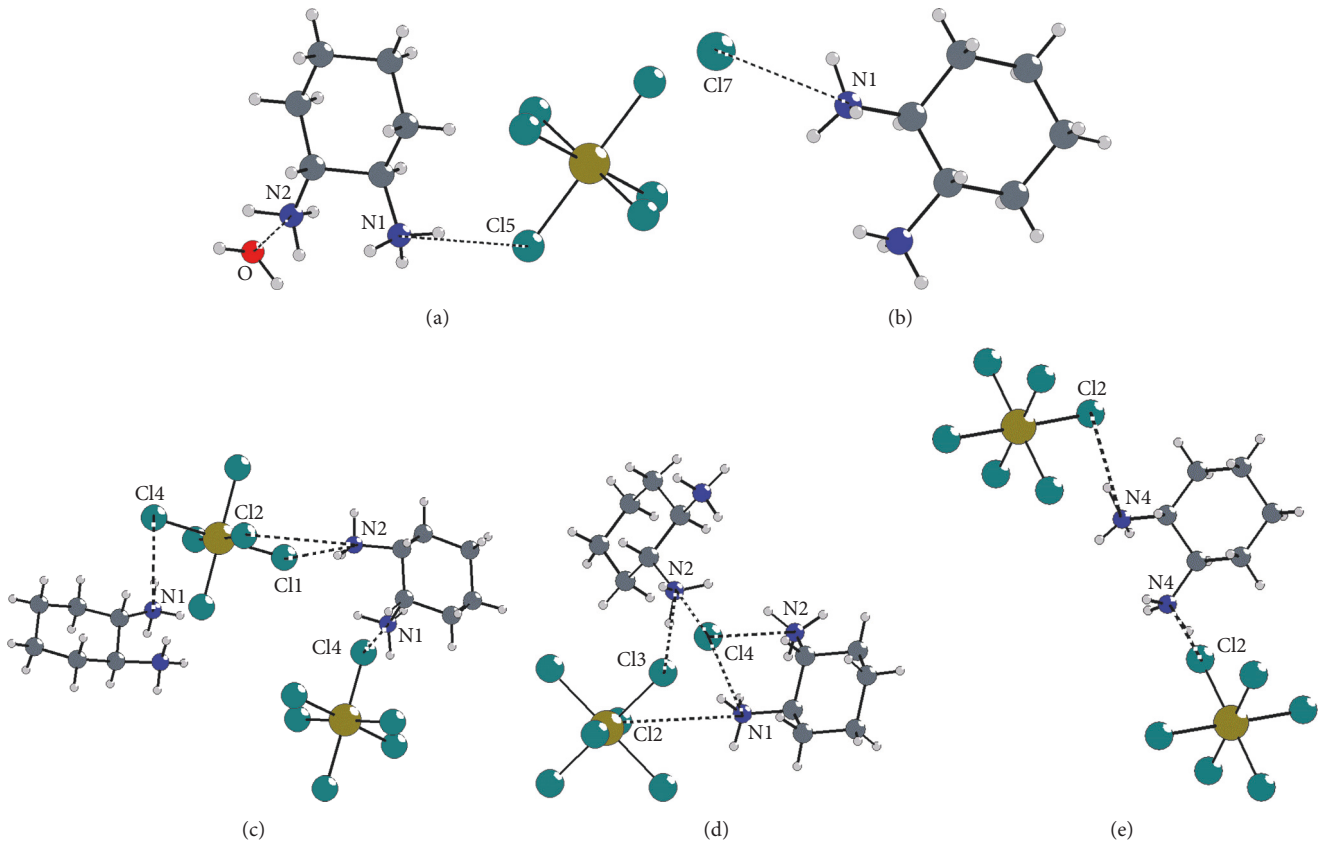

Figure 6: Configuration of hydrogen bonds in the studied compounds. (a) $C_6H_{10}(NH_3)_2[PtCl_6]\cdot H_2O$ **(I)**, (b) $C_6H_{10}(NH_3)_2[PtCl_6]\cdot 2HCl$ **(II)**, (c) $C_6H_{10}(NH_3)_2[PtCl_6]$ **(III)**, (d) $(C_6H_{10}(NH_3)_2)_2[PtCl_6]Cl_2$ **(V)**, and (e) $C_6H_{10}(NH_3)_2[PtCl_6]\cdot HCl$ **(VI)**.

solvent. Seven new phases were obtained. The phases can be used as precursors for tetraplatin synthesis. Some crystal phases contain H_2O or HCl molecules stabilizing the structure. The crystal structures of the five crystalline phases were determined using X-ray powder diffraction technique. It is relevant to mention that powder diffraction technique was only possible in this investigation because of principal inaccessibility of single crystal samples. The ions $[PtCl_6]^{2-}$ and 1,2-$C_6H_{10}(NH_3)_2^{2+}$ connected by hydrogen bonds are packed in crystal structures. The diversity of crystal phases relates to specific ions sizes, shapes, symmetry and charge distribution, spatial configuration of acceptors, and donors of hydrogen bonds. It results in specific configuration of hydrogen bonds which seems to be formed in solution providing association of the ions into various groups. The varied solution conditions promote crystallization of solid phases with different crystal structures. The obtained phases are comparable on the thermal stability. They are stable up to 373 K in air. The thermal decomposition occurs in several stages, accompanied by the removal of organic and solvate parts with consistent formation of platinum chloride compounds. The discussed crystallization phenomena have a practical usefulness for development of new approaches for synthesis of important drugs.

Conflicts of Interest

The authors declare that they have no conflicts of interest.

Acknowledgments

The study was performed in Siberian Federal University in accordance with the 2014–2016 years' government order from the Ministry of Science and Education of the Russian Federation, Projects 3049 and 3098, Item 1025. The authors also acknowledge "Fund for Assistance to Small Innovative Enterprises in Science and Technology" (Grant Program "UMNIK" 2013 II half GU1/2014), ICDD Grant-in-Aid, no. 93-10 for financial support.

References

[1] F. H. Allen, "The cambridge structural database: a quarter of a million crystal structures and rising," *Acta Crystallographica Section B: Structural Science*, vol. 58, no. 3, pp. 380–388, 2002.

[2] O. Rixe, W. Ortuzar, M. Alvarez et al., "Oxaliplatin, tetraplatin, cisplatin, and carboplatin: spectrum of activity in drug-resistant cell lines and in the cell lines of the national cancer institute's anticancer drug screen panel," *Biochemical Pharmacology*, vol. 52, no. 12, pp. 1855–1865, 1996.

[3] G. R. Gibbons, S. Wyrick, and S. G. Chaney, "Rapid reduction of tetrachloro(d,l-trans)l,2-diaminocyclohexaneplatinum(IV) (tetraplatin) in RPMI 1640 tissue culture medium," *Cancer Research*, vol. 49, no. 6, pp. 1402–1407, 1989.

[4] E. Alessio, *Bioinorganic Medical Chemistry*, Wiley-VCH, Weinheim, Germany, 2011.

[5] A. Bhargava and U. N. Vaishampayan, "Satraplatin: leading the new generation of oral platinum agents," *Expert Opinion on Investigational Drugs*, vol. 18, no. 11, pp. 1787–1797, 2009.

[6] E. R. Guggenheim, D. Xu, C. X. Zhang, P. V. Chang, and S. J. Lippard, "Photoaffinity isolation and identification of proteins in cancer cell extracts that bind to platinum-modified DNA," *ChemBioChem*, vol. 10, no. 1, pp. 141–157, 2009.

[7] S. M. Aris and N. P. Farrell, "Towards antitumor active trans-platinum compounds," *European Journal of Inorganic Chemistry*, no. 10, pp. 1293–1302, 2009.

[8] V. Amani, R. Rahimi, and H. R. Khavasi, "Bis(2,6-dimethylpyridinium) hexa-chlorido-platinate(IV)," *Acta Crystallographica Section E: Structure Reports Online*, vol. 64, no. 9, pp. m1143–m1144, 2008.

[9] S. J. Sabounchei, P. Shahriary, Y. Gholiee, S. Salehzadeh, H. R. Khavasi, and A. Chehregani, "Platinum and palladium complexes with 5-methyl-5-(2-pyridyl)-2,4- imidazolidenedione: Synthesis, crystal and molecular structure, theoretical study, and pharmacological investigation," *Inorganica Chimica Acta*, vol. 409, pp. 265–275, 2014.

[10] J. H. K. A. Acquaye and M. F. Richardson, "Palladium and platinum complexes with vitamin B6 compounds," *Inorganica Chimica Acta*, vol. 201, no. 1, pp. 101–107, 1992.

[11] U. Jungwirth, C. R. Kowol, B. K. Keppler, C. G. Hartinger, W. Berger, and P. Heffeter, "Anticancer activity of metal complexes: involvement of redox processes," *Antioxidants and Redox Signaling*, vol. 15, no. 4, pp. 1085–1127, 2011.

[12] E. Reisner, V. B. Arion, B. K. Keppler, and A. J. L. Pombeiro, "Electron-transfer activated metal-based anticancer drugs," *Inorganica Chimica Acta*, vol. 361, no. 6, pp. 1569–1583, 2008.

[13] A. S. Gaballa, H. Schmidt, C. Wagner, and D. Steinborn, "Structure and characterization of platinum(II) and platinum(IV) complexes with protonated nucleobase ligands," *Inorganica Chimica Acta*, vol. 361, no. 7, pp. 2070–2080, 2008.

[14] D. Gibson, "The mechanism of action of platinum anticancer agents - What do we really know about it?" *Dalton Transactions*, no. 48, pp. 10681–10689, 2009.

[15] M. S. Ali, S. R. Ali Khan, H. Ojima et al., "Model platinum nucleobase and nucleoside complexes and antitumor activity: X-ray crystal structure of [PtIV(trans-1R,2R-diaminocyclohexane) trans-(acetate)2(9-ethylguanine)Cl]NO3·H2O," *Journal of Inorganic Biochemistry*, vol. 99, no. 3, pp. 795–804, 2005.

[16] H. Kwang, "Diacridinium hexachloridoplatinate(IV) dehydrate," *Acta Crystallographyca. Section E*, vol. 66, 425 pages, 2010.

[17] J. Yang, W. Liu, M. Sui, J. Tang, and Y. Shen, "Platinum (IV)-coordinate polymers as intracellular reduction-responsive backbone-type conjugates for cancer drug delivery," *Biomaterials*, vol. 32, no. 34, pp. 9136–9143, 2011.

[18] L. Kelland, "The resurgence of platinum-based cancer chemotherapy," *Nature Reviews Cancer*, vol. 7, no. 8, pp. 573–584, 2007.

[19] M. R. Müller, K. A. Wright, and P. R. Twentyman, "Differential properties of cisplatin and tetraplatin with respect to cytotoxicity and perturbation of cellular glutathione levels," *Cancer Chemotherapy and Pharmacology*, vol. 28, no. 4, pp. 273–276, 1991.

[20] L. R. Kelland, S. Y. Sharp, C. F. O'Neill, F. I. Raynaud, P. J. Beale, and I. R. Judson, "Mini-review: discovery and development of platinum complexes designed to circumvent cisplatin resistance," *Journal of Inorganic Biochemistry*, vol. 77, no. 1-2, pp. 111–115, 1999.

[21] G. Eastland Jr., "Tetraplatin," *Drugs of the Future*, vol. 12, no. 2, pp. 139–141, 1987.

[22] S. D. Wyrick and S. G. Chaney, "Synthesis of [^{195}mPt]-tetraplatin," *Journal of Labelled Compounds and Radiopharmaceuticals*, vol. 28, no. 7, pp. 753–756, 1990.

[23] A. K. Starkov, R. F. Mulagaleev, and S. D. Kirik, "Preparation of trans-1,2-diaminocyclohexanetetrachloroplatinum(IV)," *Russian Journal of Coordination Chemistry*, vol. 37, no. 9, pp. 718-718, 2011.

[24] R. F. Mulagaleev, A. K. Starkov, and S. D. Kirik, "A method for preparing trans-1,2-diamine cyclohexane tetra chlorine platinum(IV)," RU Patent No.2457838.

[25] C. E. S. Bernardes, M. L. S. M. Lopes, J. R. Ascenso, and M. E. M. Da Piedade, "From molecules to crystals: the solvent plays an active role throughout the nucleation pathway of molecular organic crystals," *Crystal Growth and Design*, vol. 14, no. 11, pp. 5436–5441, 2014.

[26] S. D. Kirik, A. K. Starkov, A. N. Matsulev, and A. A. Kondrasenko, "Two crystal forms of cis-bis(ethylamine) dichloro platinum(II)," *Journal of Molecular Structure*, vol. 987, no. 1-3, pp. 152–157, 2011.

[27] R. F. Mulagaleev and S. D. Kirik, "Palladium acetate: preparation and molecular scheme of synthesis," *Journal of Applied Chemistry*, vol. 83, no. 12, pp. 1937–1947, 2010.

[28] S. D. Kirik, A. K. Starkov, and R. F. Mulagaleev, "New approaches to synthesis of platinum complexes with bioactivity," in *Chemistry for Sustainable Development*, pp. 261–267, Chemistry for sustainable development, 3rd edition, 2010.

[29] S. D. Kirik, R. F. Mulagaleev, and A. L. Blokhin, "[Pd(CH3COO)2]n from X-ray powder diffraction data," *Acta Crystallographica Section C: Crystal Structure Communications*, vol. 60, no. 9, pp. m449–m450, 2004.

[30] S. D. Kirik, R. F. Mulagaleev, and A. I. Blokhin, "$[Pd_8(CH_3COO)_8(NO)_8]$: solution from X-ray powder diffraction data," *Acta Crystallographica Section C: Crystal Structure Communications*, vol. 61, no. 10, pp. m445–m447, 2005.

[31] S. I. Ginzburg, N. A. Ezerskaya, I. V. Prokofiev, N. V. Fedorenko, V. I. Shlenskaya, and N. K. Belsky, *Analytical Chemistry of Platinum Metals*, Nauka, Moscow, Russia, 1972.

[32] A. L. Spek, "Structure validation in chemical crystallography," *Acta Crystallographica D*, vol. 65, no. 2, pp. 148–155, 2009.

[33] A. Weissberger, E. S. Proskauer, J. A. Riddick, and E. E. Toops, *Organic Solvents*, Interscience Publisher, New York, NY, USA, 1955.

[34] I. I. Cherniayev, *Manual for Syntheses of the Platinum Group Metal Compounds*, M. Science, 1964.

[35] J. W. Visser, "Fully automatic program for finding the unit cell from powder data," *Journal of Applied Crystallography*, vol. 2, no. 3, pp. 89–95, 1969.

[36] S. D. Kirik, S. V. Borisov, and V. E. Fedorov, "Symmetry independent algoriphm for indexing of X-ray powder pattern," *Zhurnal. Strukturnoi. Khimii*, vol. 22, pp. 131–135, 1981 (Russian).

[37] L. Solovyov and S. Kirik, "Application of a simulated annealing approach in powder crystal structure analysis," *Materials Science Forum*, vol. 133-136, pp. 195–200, 1993.

[38] V. Favre-Nicolin and R. Černý, "FOX, 'free objects for crystallography': a modular approach to ab initio structure determination from powder diffraction," *Journal of Applied Crystallography*, vol. 35, no. 6, pp. 734–743, 2002.

[39] J. Rodriguez-Carvajal, *FullProf Version 4.06*, ILL, USA, 2009, http://www.ccp14.ac.uk/tutorial/fullprof/doc/fp_text.htm.

[40] S. D. Kirik, "Refinement of the crystal structures along the powder pattern profile by using rigid structural constraints," *Kristallographia*, vol. 30, pp. 185–187, 1985 (Russian).

[41] V. E. Fedorov, V. K. Evstafyev, S. D. Kirik, and A. V. Mischenko, "Synthesis, structure and properties of the novel niobium chalcohalides NbXY," *Russian Journal of Inorganic Chemistry*, vol. 26, no. 10, pp. 2701–2707, 1981 (Russian).

[42] Siemens, *XP. Molecular Graphics Program. Version 4.0*, Siemens Analytical X-ray Instruments Inc., Madison, Wis, USA, 1989.

[43] K. Nakamoto, *Infrared and Raman Spectra of Inorganic and Coordination Compounds: Part B: Applications in Coordination, Organometallic, and Bioinorganic Chemistry*, Wiley, 2009.